

Quantum Critical Behavior of Electrons at the Edge of Charge Order

L. Cano-Cortés,¹ J. Merino,¹ and S. Fratini²

¹*Departamento de Física Teórica de la Materia Condensada, Universidad Autónoma de Madrid, Madrid 28049, Spain*

²*Institut Néel–CNRS and Université Joseph Fourier, Boîte Postale 166, F-38042 Grenoble Cedex 9, France*

(Received 12 May 2010; published 16 July 2010)

We consider quantum critical points in which quantum fluctuations associated with charge rather than magnetic order induce unconventional metallic properties. Based on finite- T calculations on a two-dimensional extended Hubbard model, we show how the coherence scale T^* characteristic of Fermi liquid behavior of the homogeneous metal vanishes at the onset of charge order. A strong effective mass enhancement reminiscent of heavy fermion behavior indicates the possible destruction of quasiparticles at the quantum critical points. Experimental probes on quarter-filled layered organic materials are proposed for unveiling the behavior of electrons across the quantum critical region.

DOI: 10.1103/PhysRevLett.105.036405

PACS numbers: 71.10.Hf, 71.10.Fd, 74.40.Kb, 74.70.Kn

Introduction.—Quantum critical points (QCPs) occur at zero-temperature second order phase transitions in which the strength of quantum fluctuations is controlled by an external field such as pressure, magnetic field, or chemical composition [1]. In recent years intensive studies have focused on itinerant electrons at the edge of magnetic order being the heavy fermion materials [2–4] prototypical examples. Much less explored but equally interesting are QCPs arising from tuning the electrons close to a charge ordering instability. This situation is realized in the quarter-filled families of layered organic superconductors [5] of the α , β'' , and θ -(BEDT-TTF)₂X types. Large electron effective mass enhancements and non-Fermi liquid metallicity at finite T are observed in (MeDH-TTP)₂AsF₆ and κ -(DHDA-TTP)₂SbF₆ above a critical pressure at which the charge order found at ambient pressure melts [6,7]. Such heavy fermion behavior may appear puzzling, considering the different π orbitals of the organics as compared to the f orbitals in the rare earths, but can find a natural explanation based on the universal properties of matter expected near a QCP.

Charge ordering (CO) phenomena in quarter-filled layered organic materials are observed in a wide variety of crystal structures, not limited to specific Fermi surface shapes or nesting. This indicates the importance of on-site and intersite Coulomb repulsion [8,9] between π electrons as the driving force of CO, and in turn implies that electronic correlation effects similar to those found in half-filled systems are inevitably present. These should be considered together with the quantum critical fluctuations of the order parameter to understand the metallic properties in the neighborhood of the present Coulomb-driven transition. The latter can, in principle, differ from more standard charge density wave instabilities of the Fermi surface.

In this Letter we analyze theoretically the possible existence of a QCP at a CO transition driven by the quantum fluctuations associated with strong off-site Coulomb repulsion, in the absence of Fermi surface nesting. The influence

of the $T = 0$ singular quantum critical point on the finite temperature metallic properties is studied based on finite- T Lanczos diagonalization [10,11] of an extended Hubbard model on an anisotropic triangular lattice. At quarter filling ($n = 1/2$ hole per molecule), lattice frustration naturally leads to charge ordered metallic states with a single CO pattern. Our main result is the existence of a temperature scale T^* in the dynamical and thermodynamic properties of the system, which is suppressed as the CO transition is approached from the homogeneous metal. The electronic specific heat coefficient at low temperatures is found to be strongly enhanced close to the QCP in analogy with studies of quantum criticality in heavy fermions. Following this analogy, non-Fermi liquid behavior should occur at finite T in quarter-filled organic conductors at the edge of a CO instability and could be directly probed by several experimentally measurable quantities. Because of the universal character of the proposed quantum critical scenario, our results could also be relevant to broader classes of systems where Coulomb-driven CO occurs, not restricted to the particular ordering pattern studied here.

Model.—We focus on the extended Hubbard model,

$$H = \sum_{\langle ij \rangle \sigma} t_{ij} (c_{i\sigma}^\dagger c_{j\sigma} + \text{H.c.}) + U \sum_i n_{i\uparrow} n_{i\downarrow} + \sum_{\langle ij \rangle} V_{ij} n_i n_j, \quad (1)$$

on the anisotropic triangular lattice shown in Fig. 1(a), where $t_{ij} = (t_p, t_c)$ are the transfer integrals between nearest neighboring molecules, respectively, along the diagonal (p) and vertical (c) directions, $V_{ij} = (V_p, V_c)$ are the corresponding intermolecular Coulomb interaction energies, and U is the intramolecular Coulomb repulsion. The model Eq. (1) has been studied via a variety of techniques due to its relevance to θ -type two-dimensional organic conductors (see Ref. [12] for a recent review). Here we follow the standard practice and neglect longer-range Coulomb interactions [12] as well as electron-lattice effects [13] that are however essential to recover the various ordering patterns

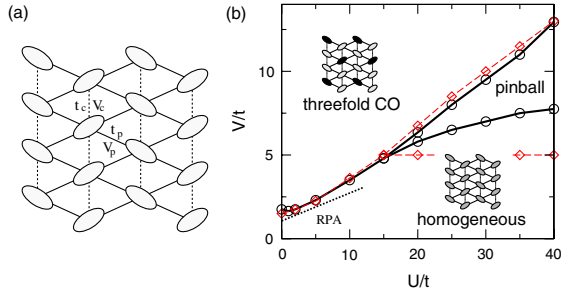


FIG. 1 (color online). (a) Lattice structure and microscopic parameters of the extended Hubbard model Eq. (1). (b) Phase diagram obtained at $T = 0$ from numerical diagonalization of $N_s = 12$ (solid line) and 18 sites clusters (dashed line). RPA is the random phase approximation.

realized in these materials. For the sake of simplicity we consider an isotropic intersite repulsion $V_c = V_p \equiv V$ and set $t_c = 0$, $t_p \equiv t > 0$. This choice is representative of the θ -ET₂X salts with $X = \text{CsCo}(\text{SCN})_4$, $X = \text{CsZn}(\text{SCN})_4$, and $X = I_3$ where the molecular orbital overlap is strongly suppressed along the c direction [8,12]. These materials lie close to (on both sides of) the bandwidth controlled CO transition in Mori’s phase diagram [8] and are therefore optimal candidates for the observation of an interplay between critical charge fluctuations and electronic correlation effects.

Phase diagram.—The phase diagram obtained at $T = 0$ from the numerical diagonalization of the model Eq. (1) on $N_s = 12$ and $N_s = 18$ site clusters is presented in Fig. 1(b). The different phases can be identified by analyzing the behavior of the charge correlation function $N_s C(\mathbf{q}) = N_s^{-1} \sum_{ij} \langle n_i n_j \rangle e^{i\mathbf{q} \cdot \mathbf{R}_{ij}}$. In the thermodynamic limit, this quantity diverges at a single wave vector $\mathbf{Q} \neq 0$ at the onset of charge order. An accurate numerical determination of the phase boundaries relying on a proper finite-size scaling of the results is prohibitive for the fermionic system under study, due to the rapidly increasing size of the Hilbert space. We therefore identify the $T = 0$ ordering transition, V_{CO} , as the locus of steepest variation of charge correlations upon varying the interaction parameters. An analogous procedure is used to determine the melting temperature of CO, T_{CO} . In the physically relevant regime explored here, $U/t \lesssim 20$ [14], the phase boundaries agree on the two cluster sizes.

In the absence of nearest-neighbor repulsion, $V = 0$, the system remains in a homogeneous metallic phase up to arbitrary values of the local interaction, U , as holes can effectively avoid each other at concentrations away from integer fillings. An instability towards a charge ordered state with threefold periodicity is realized instead upon increasing the intersite interaction, V , as was previously obtained by different approaches [12,15–19]. The resulting threefold ordering pattern is shown in Fig. 1(b).

At low and moderate values of $U/t \lesssim 5$, down to $U = 0$, the CO transition essentially follows the predictions of

mean-field approaches [12,15,16]. A calculation in the random phase approximation yields $V_{\text{CO}} = 1.06t + U/6$, which is shown as a dotted line in Fig. 1(b). This law is correctly recovered by the numerical data at low U , but sizable deviations appear as soon as $U/t \gtrsim 10$ due to the increasing effects of many-body electronic correlations. The boundary obtained numerically in this region is independent of the cluster size, and our value $V_{\text{CO}}/t = 3.5$ at $U/t = 10$ is in good agreement with existing numerical results in larger systems [18,19].

Before moving to the analysis of the correlated metallic phase at the edge of charge order, let us note that the charge correlation function also provides indications of a cross-over taking place within the CO phase, separating a conventional threefold state from a more exotic “pinball liquid” phase [17]. The latter arises because at large U , mean-field like configurations where charge-poor molecules are completely depleted become energetically unfavorable, as these imply that each charge rich molecule should accommodate up to $3/2$ holes on average. To prevent double occupancy, part of the hole density necessarily spills out and decouples from the charge rich sublattice, resulting in a separate fluid moving freely in the remaining sublattice [17]. This partial ordering, occurring for $V \leq U/3$, corresponds to a value $C(\mathbf{Q}) = n^2/3$, to be contrasted with the value $C(\mathbf{Q}) = n^2$ obtained in the threefold state at large V .

The correlated metal close to charge ordering.—We start by analyzing the kinetic energy of the interacting system, a quantity that provides direct information on how the motion of the charge carriers is hindered by interactions, and can be evaluated with good accuracy through finite- T Lanczos diagonalization. Its importance in correlated systems has been recently recognized [20,21], and resides in the fact that it can in principle be accessed from optical absorption experiments, providing a quantitative measure of many-body correlation effects.

The kinetic energy, K , normalized to the noninteracting band value, K_0 , is shown in Figs. 2(a) and 2(b), respectively, for $U/t = 5$ and $U/t = 15$, for several values of the intersite repulsion across the CO transition. At $U/t = 5$ the kinetic energy at $T = 0$ stays essentially unrenormalized, $K/K_0 \gtrsim 0.9$, upon increasing V all the way up to the CO transition occurring at $V_{\text{CO}} = 2.33t$, as expected in a weakly correlated Fermi liquid. It then suddenly drops to a value $K/K_0 \sim 0.6$ upon entering the charge ordered phase. This residual value is ascribed to local (incoherent) hopping processes in the charge ordered pattern [20] and to the motion of remnant itinerant electrons not gapped by the ordering transition [16,18].

A richer behavior is revealed by the data at finite temperatures, which clearly indicates the emergence of a temperature scale T^* that marks an analogous suppression of the kinetic energy occurring within the homogeneous metallic phase (we define T^* as the locus of steepest variation of K with temperature, denoted by arrows in Fig. 2). The scale T^* appears to be entirely controlled by

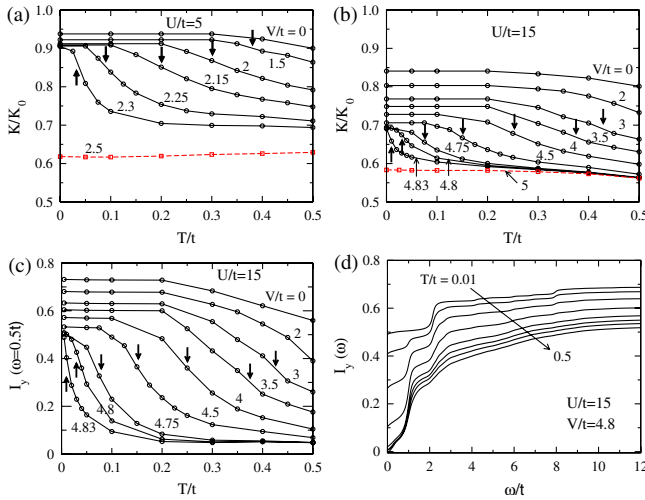


FIG. 2 (color online). Kinetic energy of the $N_s = 12$ interacting system at $U/t = 5$ (a) and $U/t = 15$ (b); T dependence of low-frequency optical weight (c), and integrated optical spectral weight $I(\omega)$ for $T/t = 0.01, 0.03, 0.05$, and $0.1-0.5$ in 0.1 intervals (d). Arrows in (a), (b), (c) correspond to inflection points of the curves, defining the temperature scale T^* .

the approach to the zero-temperature ordering transition, a behavior that is strongly reminiscent of what is expected close to a QCP. The situation is similar at $U/t = 5$ and $U/t = 15$ [Fig. 2(b)], although in the latter case the kinetic energy ratio at $T = 0$ is already reduced down to values $K/K_0 \sim 0.7$ before entering the CO phase at $V_{CO} = 4.83t$, which is indicative of a moderately correlated electron liquid. In this case the quantum critical behavior adds up to the correlated electron picture, affecting the motion of electrons that have already been slowed down by local electronic correlations.

The above observations can be directly related to the low-energy quasiparticle properties by analyzing the temperature dependence of the integrated optical weight $I(\omega) = \int_0^\omega \sigma(\omega') d\omega'$. The low-frequency integral $I(\omega = 0.5t)$, reported in Fig. 2(c), comprises most of the quasiparticles contributing to the Drude behavior in a normal Fermi liquid, while excluding higher-energy incoherent excitations arising from the strong electronic interactions. Comparison of Figs. 2(b) and 2(c) demonstrates that the strong reduction of kinetic energy above T^* primarily originates from a drastic suppression of the low-energy coherent quasiparticles. Finally, Fig. 2(d) illustrates $I(\omega)$ at a given $V/t = 4.8$ just below the CO transition, showing that the quasiparticle weight lost at T^* is partly transferred to high-energy excitations, which are broadly distributed on the scale of U, V .

The above results are summarized in the finite temperature phase diagram of Fig. 3, which constitutes the central result of this work. Scaled units V/V_{CO} are used so that the weakly ($U/t = 5$) and moderately ($U/t = 15$) correlated cases can be directly compared, illustrating the universality of the T^* phenomenon in proximity to the CO instability.

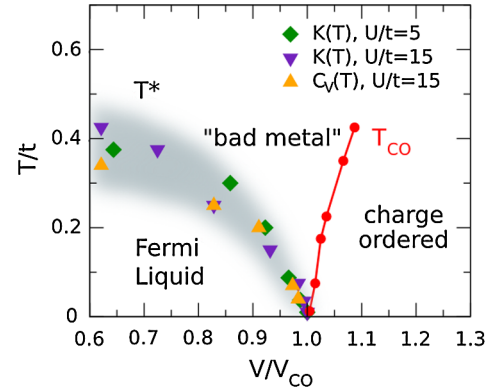


FIG. 3 (color online). Finite temperature phase diagram illustrating the emergence of non-Fermi liquid properties induced by the proximity to the charge ordering transition. The interaction strength has been rescaled to the critical values to compare QCP related properties for weakly and moderately correlated systems.

Both T^* and T_{CO} appear to vanish at V_{CO} , leading to a funnel-type “bad” metallic region with strong quantum critical fluctuations.

To obtain further insight into the behavior of quasiparticles near the CO instability and make contact with the established concepts of quantum criticality, we have calculated the specific heat coefficient $\gamma = C_V/T$. Our results, reported in Fig. 4(a), resemble the behavior of nearly two-dimensional antiferromagnetic metals in which a singular increase is expected upon lowering the temperature close to the QCP, crossing over to a constant value at the onset of Fermi liquid behavior [4,22]. Curves similar to those in Fig. 4(a) are commonly observed in heavy fermion systems [4,23,24]. As a striking confirmation of the QCP scenario emerging from the preceding paragraphs, we see that there is a direct correspondence between thermodynamic and dynamical properties: the peak position in the specific heat essentially coincides with the temperature T^* derived from the kinetic energy and the low-frequency optical integral near to the QCP (see Fig. 3).

Finally, we discuss the behavior of the effective mass as extracted from the low-temperature limit of the specific heat coefficient (in practice we estimate m^* from the peak value of γ to overcome the numerical limitations of the Lanczos technique at low T). It can be expected on general grounds that the strong electron-electron interactions responsible for the threefold CO will strongly affect those parts of the Fermi surface that are connected by momenta closest to the ordering wave vector \mathbf{Q} . This should lead to the emergence of “hot spots” with divergent effective mass, $m^*/m_b \propto \ln(1/|V - V_{CO}|)$, in full analogy to the situation encountered in metals close to a magnetic instability [22,25]. The effective mass reported in Fig. 4(b) indeed shows a marked enhancement at the approach of V_{CO} , which adds to a moderate renormalization $m^*/m_b \lesssim 2$ provided by noncritical electronic correlations. Whether the destruction of quasiparticles remains confined to such “hot spots” or spreads over the whole Fermi surface is an

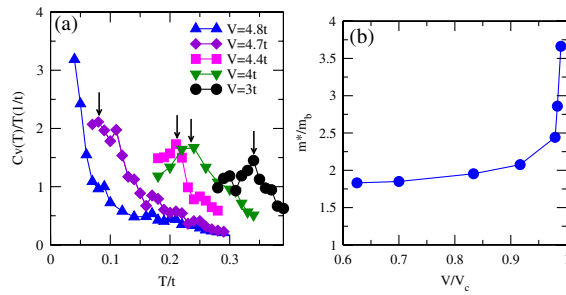


FIG. 4 (color online). (a) Specific heat coefficient $\gamma = C_V/T$ in units of $1/t$ for $U/t = 15$. The curves are shown down to a temperature comprising ~ 10 excitations in the Lanczos diagonalization. (b) Effective mass ratio, m^*/m_b , estimated from the peak value of γ shown in (a).

unsettled issue that is also actively debated in the context of heavy fermion materials [2,3].

Concluding remarks.—Our results indicate the occurrence of non-Fermi liquid behavior driven by a combination of electronic correlations and quantum critical fluctuations close to a CO instability in quarter-filled organic conductors. Quantum critical behavior has been recently reported in transport studies of the quarter-filled compounds κ -(DHDA-TTP) $_2$ SbF $_6$ and (MeDH-TTP) $_2$ AsF $_6$, by tuning the system across the CO transition via an applied pressure [6,7]. A stringent verification of our theoretical predictions could be achieved in the conductor θ -(BEDT-TTF) $_2$ I $_3$, whose band structure is properly described by the model Eq. (1). Remarkably, this is the only salt of the θ family exhibiting superconductivity and is at the edge of CO. Recent optical studies [26] have shown a rapid loss of electron coherence upon increasing the temperature, associated with a marked reduction of kinetic energy as obtained here, and the evolution of the integrated spectral weight $I(\omega)$ with temperature found experimentally compares very well with our result in Fig. 2(d). The presence of an unexplained far infrared absorption peak whose position is controlled by the temperature scale T alone could be a clue of an emergent collective excitation of the QCP [27]. This material undergoes a CO transition under pressure [28], which could be directly exploited to probe the quantum critical behavior, applying the plethora of experimental techniques that are commonly used in the study of heavy fermion materials. Hall coefficient as well as de Haas–van Alphen experiments appear to be ideal probes to test whether quasiparticles are destroyed over the whole Fermi surface or on some regions only, shedding light on the nature of the charge order QCP.

L.C. and J.M. acknowledge financial support from MICINN (CTQ2008-06720-C02-02, CSD2007-00010),

and computer resources and assistance provided by BSC. The authors thank I. Paul for useful discussions.

- [1] S. Sachdev, *Quantum Phase Transitions* (Cambridge University Press, Cambridge, England, 2001).
- [2] P. Coleman, *Handbook of Magnetism and Advanced Magnetic Materials* (Wiley, New York, 2007), Vol. 1, p. 95.
- [3] P. Gegenwart, Q. Si, and F. Steglich, *Nature Phys.* **4**, 186 (2008).
- [4] H. v. Löhneysen *et al.*, *Rev. Mod. Phys.* **79**, 1015 (2007).
- [5] T. Ishiguro, K. Yamaji, and G. Saito, *Organic Superconductors* (Springer, New York, 2001), 2nd. ed.
- [6] S. Yasuzuka *et al.*, *J. Phys. Soc. Jpn.* **75**, 083 710 (2006).
- [7] Y. Weng *et al.*, *Synth. Met.* **159**, 2394 (2009).
- [8] H. Mori, S. Tanaka, and T. Mori, *Phys. Rev. B* **57**, 12 023 (1998).
- [9] R.H. McKenzie *et al.*, *Phys. Rev. B* **64**, 085109 (2001).
- [10] J. Jaklič and P. Prelovšek, *Phys. Rev. B* **49**, 5065 (1994).
- [11] We use an Arnoldi algorithm: see A. Liebsch, H. Ishida, and J. Merino, *Phys. Rev. B* **78**, 165123 (2008).
- [12] K. Kuroki, *Sci. Tech. Adv. Mater.* **10**, 024 312 (2009).
- [13] M. Udagawa and Y. Motome, *Phys. Rev. Lett.* **98**, 206405 (2007).
- [14] Values of $U \approx 10t$ and $V \approx 2t$ were estimated from optical reflectivity data in T. Mori, *Bull. Chem. Soc. Jpn.* **73**, 2243 (2000), whereas a larger $U \approx 20t$ is extracted from the density-functional theory bare value U_0 with a screening reduction of $U \sim U_0/2$ with $t = 0.1$ eV; E. Scriven and B.J. Powell, *J. Chem. Phys.* **130**, 104 508 (2009); L. Cano-Cortés *et al.*, *Eur. Phys. J. B* **56**, 173 (2007).
- [15] T. Mori, *J. Phys. Soc. Jpn.* **72**, 1469 (2003).
- [16] M. Kaneko and M. Ogata, *J. Phys. Soc. Jpn.* **75**, 014 710 (2006).
- [17] C. Hotta and N. Furukawa, *Phys. Rev. B* **74**, 193107 (2006).
- [18] H. Watanabe and M. Ogata, *J. Phys. Soc. Jpn.* **75**, 063 702 (2006).
- [19] S. Nishimoto, M. Shingai, and Y. Ohta, *Phys. Rev. B* **78**, 035113 (2008).
- [20] A.J. Millis, in *Strong Interactions in Low Dimensions*, edited by D. Baeriswyl and L. DeGiorgi (Springer Verlag, Berlin, 2004).
- [21] M.M. Qazilbash *et al.*, *Nature Phys.* **5**, 647 (2009).
- [22] T. Moriya and K. Ueda, *Adv. Phys.* **49**, 555 (2000).
- [23] G.R. Stewart *Rev. Mod. Phys.* **56**, 755 (1984); **73**, 797 (2001).
- [24] J. Custers *et al.*, *Nature (London)* **424**, 524 (2003).
- [25] J. Merino *et al.*, *Phys. Rev. Lett.* **96**, 216402 (2006).
- [26] K. Takenaka *et al.*, *Phys. Rev. Lett.* **95**, 227801 (2005).
- [27] S. Caprara, *et al.*, *Phys. Rev. Lett.* **88**, 147001 (2002); **75**, 140505(R) (2007).
- [28] N. Tajima *et al.*, *J. Phys. IV* **114**, 263 (2004).